U.S. DEPARTMENT OF THE INTERIOR
U.S. GEOLOGICAL SURVEY

$^{40}Ar/^{39}Ar$ Ages of Volcanic Rocks from offshore Southern and Peninsular California and the Southern California Borderland

by

Wendy A. Bohrson[1] and Alicé S. Davis[2]

Open-File Report 94- 587

[1]Present address: Department of Geological Sciences,
University of California, Santa Barbara, CA 93106-1100

[2]U.S. Geological Survey, MS-999
Menlo Park , CA 94025

Introduction

There is an abundance of volcanic edifices offshore southern and peninsular California (Fig. 1). Morphologically these edifices are diverse, ranging from small conical volcanoes to large, complex volcanic ridges. Many volcanic edifices are isolated, others are clustered, and some occur in short linear chains which appear to be aligned NW-SE, parallel to plate motion, or NE-SW, nearly orthogonal to the direction of plate motion. The origin of most of these features and their relationships to the regional tectonic history are poorly understood. Radiometric age data for southern and peninsular California are sparse, and more studies are needed to clarify age distribution. The most comprehensive age study is that for Jasper Seamount, offshore southern California; comprising 29 laser total fusion $^{40}Ar/^{39}Ar$ ages ranging from about 10 to 4 Ma (Pringle and others, 1991). Ages for Guadalupe Island, offshore northern Baja, (Batiza, 1977 a, b; Batiza and others, 1979) include one conventional K-Ar age of 7.2 Ma and two $^{40}Ar/^{39}Ar$ incremental heating ages of 5.4 and 3.4 Ma. Other ages published for seamounts in this region include one conventional whole-rock K-Ar age of 20.3 ±1.4 Ma for an alkalic basalt from the summit of Fieberling Guyot (Lonsdale, 1991) and a $^{40}Ar/^{39}Ar$ incremental heating age of 7.8 ±0.8 Ma for Henderson Seamount (Honda and others, 1987). A conventional K-Ar age of 4.36 ±0.8 Ma, determined for basalt from Northeast Bank, at the outer margins of the California Borderland, is in agreement with a fission track age of 4.5 ±0.5 Ma, determined for basaltic glass from the same site (Hawkins and others, 1971).

This report presents results of $^{40}Ar/^{39}Ar$ laser fusion analyses for 7 plagioclase separates from seamounts offshore southern California, for 5 plagioclase separates from basaltic glasses from the southern California Continental Borderland, and for 1 sanidine sample from Rocas Alijos, offshore Baja.

Sampling Methods

Samples from seamounts offshore southern California were collected by dredging on U.S. Geological Survey Cruise F7-87-SC aboard the R/V *Farnella* in December, 1987. Average dredge locations are given in Table 1; detailed sampling information and glass microprobe analyses of the dredged samples are given by Davis and others (1990). The samples from the southern California Continental Borderland are glass sand or glassy pillow lava fragments recovered from dart cores on several U.S. Geological Survey cruises; details are given by Vedder and others (1990). The sample from Rocas Alijos, offshore central Baja, was collected by scuba divers on the 1990 Cordell Expedition to Rocas Alijos, and detailed sample description and whole-rock chemistry are given by Davis and others (1994).

$^{40}Ar/^{39}Ar$ analytical methods and data treatment

Feldspar separates were obtained by crushing, magnetic separation, and hand picking. Samples were ultrasonically cleaned in ~10% HF and rinsed several times in distilled water. Five to 150 mg of material were wrapped in aluminum foil and sealed in evacuated quartz (dredge samples) or Pyrex (Rocas Alijos) tubes. Fish Canyon Tuff (27.8 Ma) sanidine flux

monitors were interleaved every 1 to 1.5 cm for dredge samples and every 5 mm for the sample from Rocas Alijos. Dredge samples were irradiated for 45 hours and the Rocas Alijos sample was irradiated for 3 hours, both at the University of Michigan Ford reactor. Measured irradiation parameters for the dredge samples are $(^{40}Ar/^{39}Ar)_K$ = 0.0275, $(^{38}Ar/^{39}Ar)_K$= 0.012, $(^{36}Ar/^{37}Ar)_{Ca}$ = 0.00029, and $(^{39}Ar/^{37}Ar)_{Ca}$ =0.00070. Parameters for the 3 hour irradiation are the same except $(^{40}Ar/^{39}Ar)_K$ = 0.0 because the sample was irradiated in a borated Pyrex tube which acted as a thermal neutron shield; therefore, no nucleogenic ^{40}Ar was detected.

Mineral grains were melted using a 5W argon laser. Because aliquots larger than about 5 mg could not be fully melted by the laser, mineral separates for an individual sample were divided into 5 mg aliquots and loaded into individual holes in a copper tray. In some cases, 10 mg of material (2 holes) were melted for a single analysis in order to generate sufficient gas. Up to ten individual analyses were performed to characterize a single sample (Table 2). In most cases, one 10 mg aliquot was partially degassed at 2-2.5W to characterize the nonradiogenic (atmospheric) component. This aliquot was then fused at 5W and analyzed. This approach is similar to the "cleaning procedure" described by Pringle and others (1991).

Isotopic measurements were performed at UCLA using a VG1200S mass spectrometer that was operated in the electron multiplier mode with a gain of 150 relative to the Faraday cup. Mass spectrometer backgrounds and extraction line blanks were analyzed prior to the start of each sample. Extraction line blanks were between $2\text{-}3x10^{-16}$ mol ^{40}Ar. Backgrounds typically had the following ranges: ^{40}Ar 0.40-0.58 mV, ^{39}Ar 0.60-0.92 mV, ^{38}Ar 0.09-0.18 mV, ^{37}Ar 0.77-0.96 mV, ^{36}Ar 0.18-0.27 mV. Sensitivity was 2×10^{-17} moles/mV during the analyses, and mass discrimination was measured at 0.36%/amu. Reactive gases were removed with a SAES Ti-Zr getter, and typical gettering times were 10-15 minutes.

Because of the long delay between irradiation and analysis, plagioclase from the dredge samples contained chlorine-derived ^{36}Ar. Assessment of the amount of Cl-derived ^{36}Ar in each sample relies on the assumption that after standard corrections (e.g. background, mass discrimination, blank, K-derived, and atmospheric) are made to measured ^{38}Ar, the remaining amount is chlorine-derived ^{38}Ar. Using that amount, the $^{36}Cl/^{38}Cl$ production ratio (316), and the ^{36}Cl half-life of 3×10^5 years (Roddick, 1983), chlorine-derived ^{36}Ar was calculated. In the most extreme case (D11-2), chlorine-derived ^{36}Ar comprises 1% of the ^{36}Ar and accounting for it results in a 6% increase in age, which is within 1σ of the age calculated without the Cl correction. The Cl correction was included because its exclusion would result in minor systematic errors in both age and radiogenic yield.

All analyses for a single sample were plotted on an inverse isochron correlation diagram ($^{36}Ar/^{40}Ar$ vs $^{39}Ar/^{40}Ar$) after correcting for interfering reactions, backgrounds, and blanks. The data were regressed using the York (1969) technique. One advantage of the inverse isochron method is the composition of the nonradiogenic component is explicitly defined and is not *assumed* to be atmospheric. (For a full discussion of inverse isochrons, see McDougall and Harrison, 1988). A homogeneous population of crystals from a single sample define a well correlated linear trend where the inverse of the Y intercept represents the $^{40}Ar/^{36}Ar$ composition of the nonradiogenic (atmospheric) component and the inverse of the X intercept provides the $^{40}Ar^*/^{39}Ar_K$ (Figure 2). Using these isotopic compositions, an inverse isochron age for each sample was calculated. The mean square of weighted deviates (MSWD) provides a statistical measure by which to assess the isochron; a MSWD of < 2.5 indicates that an isochron is defined by a homogeneous population of crystals where scatter results only from experimental error (McIntyre and others, 1966, Brooks and others, 1972, Dalrymple and

Lanphere, 1974; see McDougall and Harrison, 1988 for discussion), and ages are typically considered reliable. In most of the samples reported here, when *all* analyses for an individual sample were regressed, the MSWD is > 2.5, suggesting that crystal populations were heterogeneous.

In these cases, a methodology similar to that of Spell and Harrison (1993) was adopted to assess the consequences of excluding analyses which clearly deviate from the "best-fit" inverse isochron. After deviates are excluded, the MSWD, $^{40}Ar/^{36}Ar$ of the nonradiogenic (atmospheric) component, and age are recalculated. In all cases, MSWD was reduced due to exclusion of selected analyses. Despite exclusion of some analyses, in several cases the MSWD did not fall below 2.5 because the analyses had a small range of $^{36}Ar/^{40}Ar$ and $^{39}Ar/^{40}Ar$. In these cases (which typically included relatively radiogenic samples), the weighted mean age is considered a better estimate of the age of the sample. In most cases, the inverse isochron and weighted mean ages were the same within uncertainty; this suggests that the nonradiogenic component had atmospheric $^{40}Ar/^{36}Ar$.

Analyses that deviated from the inverse isochron regression typically fell into 2 categories. Those 5W analyses that were clearly older than the best fit age were probably contaminated with xenocrysts or had excess argon. Because each analysis comprises up to 10 mg of feldspar, ages of the xenocrysts can not be assessed. The second group of outliers was the 2.0-2.5W analyses. Ages calculated for these steps were substantially older than or younger than the best fit age, and these steps had nonradiogenic components different in composition from those of the 5.0W fusions. In all cases, the group of analyses that yield the lowest MSWD for an individual sample is represented in Figure 2 and Table 3.

We used the following criteria to determine the validity of each age: inverse isochron results, evidence for excess argon or xenocrysts, comparisons between weighted mean and inverse isochron results, and the age of the underlying oceanic crust. Each sample is discussed individually in the following section.

Discussion of $^{40}Ar/^{39}Ar$ results

Dredge samples from offshore southern California yielded ages that range from ~20 to ≤ 7(?) Ma, and those from the California Borderland yielded ages between ~32 and 9 Ma. The sample from Rocas Alijos is ~270 ka. Analytical precision varied due to sample size, K abundance, and radiogenic yield (atmospheric contamination). Inverse isochron and weighted mean ages, $^{40}Ar/^{36}Ar$ composition of the nonradiogenic component, and the age of the underlying oceanic crust are summarized in Table 3.

Offshore Southern California

Seven plagioclase age determinations characterize seamounts from offshore southern California. The weighted mean age of sample D3-18 is 12.4±0.1 Ma and is probably the best age estimate for this sample. Regression of 4 analyses of D3-18 (Figure 2a) results in an inverse isochron age of 12.0±0.4 Ma. The MSWD is high (77) because the 4 analyses have a small range of $^{36}Ar/^{40}Ar$ and $^{39}Ar/^{40}Ar$. In addition, because the sample is relatively radiogenic (~80%), the dispersion in the data is magnified when the $^{40}Ar/^{36}Ar$ composition of the nonradiogenic component is extrapolated; this leads to a large uncertainty in the $^{40}Ar/^{36}Ar$ composition of the nonradiogenic component, and it is therefore not reported. However, the

similarity between the weighted mean and inverse isochron ages suggests that the composition of the nonradiogenic component is largely atmospheric. Sample D9-22 is represented by 8 analyses that yield an inverse isochron age of 16.8±0.3 Ma (Figure 2b) and a relatively low MSWD (3.4). The nonradiogenic component has a $^{40}Ar/^{36}Ar$ of 296.9±2.9, which, within uncertainty, is atmospheric. The similarity between the weighted mean age of 16.8±0.1 Ma and the inverse isochron age is an indication that the age of D9-22 is very well constrained.

Two samples have very low radiogenic yields that result in ages with large uncertainties. Most analyses of D5-20 resulted in radiogenic yields of less than 10%, yielding ages which varied widely. Because regression of this data produced an age with a large uncertainty and a large MSWD, it is considered unreliable. A low temperature heating step (1.5-2.5 W) removed some of the nonradiogenic component, thereby increasing the radiogenic yield to ~19%. This analysis (c_3) represents the best estimate of 15.8±0.8 Ma for D5-20, provided that the nonradiogenic component is atmospheric in composition ($^{40}Ar/^{36}Ar = 295.5$). Despite the increase in radiogenic yield, this result should be viewed with caution. D6-31 has low radiogenic yield, and the small sample size prevented heating aliquots at low temperature. Only one analysis of D6-31 was possible, and thus, the reported age of 11±2 Ma is limited by poor radiogenic yield and the assumption that the nonradiogenic component is atmospheric.

Analyses of D14-1 are subject to large uncertainties due, at least in part, to incomplete gettering. Between the time the gas was introduced into the mass spectrometer and initiation of the analysis (~50 seconds), the intensity of mass 40 fell 25%. Large uncertainties on other masses suggest that a similar phenomenon may have affected masses 39-36. Poor reproducibility and the drop in intensity may have been associated with the introduction of gas other than argon into the mass spectrometer (HO, H_2). In view of these complications, the ages listed for D14-1 (6.5-10.7 Ma, Table 2) should be viewed with caution.

Consistent with major and trace element chemistry, plagioclase from two samples (D11-2 and D17-28) has low K_2O abundance's (<0.10 wt %) that are characteristic of mid-ocean ridge basalt (MORB). Because of the low K contents in these samples, incorporation of excess argon can result in apparent ages that are much older than crystallization ages (e.g. Dalrymple, 1975). D11-2 yielded ages in excess of the age of the oceanic crust upon which the seamount resides, suggesting the presence of excess argon. Regression of inverse isochron data also yielded an age in excess of that of the oceanic crust. Thus, we conclude that ages for D11-2 are unreliable. D17-28 yielded ages ranging from ~11 to 30 Ma. Three analyses yielded ages ranging from 20.8 ±3.6 to 24.5 ±1.2 Ma which are close to the age of the oceanic crust (Chron 6, ~20-21 Ma); such ages would be consistent with the seamount forming near a spreading center as suggested by its MORB-like chemistry. However, two analyses deviate dramatically from this range (one at ~30 Ma, suggesting the presence of excess Ar, and one at ~11 Ma), hence, the analyses must be viewed with caution.

Southern California Continental Borderland

Southern California Continental Borderland is characterized by 5 plagioclase $^{40}Ar/^{39}Ar$ ages. Three samples (T222, T501, T503) were characterized by high radiogenic yields and precise ages. Inverse isochron ages for these ranged from 30.6±0.1 to 31.2±0.2 Ma and are comparable to weighted mean ages, which range from 30.9 to 31.5 Ma. Two samples, T222 and T503 had relatively low MSWD (3.3 and 1.68, respectively). T501 had an MSWD of 53, which reflects clustering of the $^{39}Ar/^{40}Ar$ and $^{36}Ar/^{40}Ar$ data. These samples provide definitive evidence for volcanism in the southern California Borderland between ~30.5 and 31.5 Ma.

Two additional samples from Northeast Bank yielded age ranges and argon systematics that were more variable than the 3 samples described above. Analyses of T488, which vary from ~28 to 67% $^{40}Ar^*$, range in age from 9 to 20 Ma. The inverse isochron age for T488 is 9.8±1.1 Ma; one fusion (b) and one of the step-heated analyses (e_1, e_2) yield ages different from the remaining analyses and account for the relatively poor uncertainty. With these analyses excluded, the inverse isochron age of 9.6±0.1 Ma (Figure 2c) is interpreted as the best age of T488 (MSWD = 4.0) and is similar to the weighted mean age of 9.3±0.1 Ma (excluding the same analyses). The inverse isochron age for T514, which has variable radiogenic yields (10 to 97%) is 10.6±0.1 Ma (MSWD = 185) with the 5W step from the step-heated samples excluded (Figure 2d). The weighted mean age of 11.5±0.1 includes all analyses. These two ages are different within uncertainty and should be interpreted as evidence for an eruption between ~10.5 and 11.5 Ma; uncertainties in the ages of this sample preclude a more precise estimate.

Rocas Alijos

AD91-374 has a well-constrained age of 270±16 ka (MSWD = 0.6) and varies between 28 and 37% $^{40}Ar^*$; the weighted mean age is very similar (275±1 Ka). The $^{40}Ar/^{36}Ar$ composition of the nonradiogenic component is 296.9±7.9 (Figure 2e).

Limitations associated with $^{40}Ar/^{39}Ar$ studies of submarine lavas

The presence of excess argon in two submarine samples from offshore southern California is consistent with observations made by Dalrymple and Moore (1968) for submarine basalts from Kilauea volcano, Hawaii, which gave anomalously old K-Ar ages. For samples collected at or below 2000 m, excess radiogenic argon was consistently measured and was attributed to incomplete degassing and rapid cooling. In this study, both low K samples (D11-2, D17-28) were dredged from depths greater than 2000 m and are nonvesicular, suggesting incomplete degassing. The samples also have glassy rinds indicative of rapid cooling. The similarities between these samples and those of Dalrymple and Moore (1968) suggest that argon retained during incomplete degassing and rapid cooling of submarine lavas provides an explanation for the anomalously old ages of the low K samples.

Pringle and others (1991) present dating results for Jasper seamount that illustrate the potential that the $^{40}Ar/^{39}Ar$ laser fusion technique has for young alkalic and transitional submarine basalts. They note that the technique may also provide age constraints for young mid-ocean ridge basalts as well. While several of our samples yielded acceptable ages, data from other samples illustrate some of the problems associated with $^{40}Ar/^{39}Ar$ studies of submarine samples. As noted, excess argon can dramatically increase apparent ages of low K samples and may be a particular problem of basalts erupted at depths > 2000m. In this study, low temperature heating steps (2.0-2.5 W) did not eliminate excess Ar. Low radiogenic yields (especially among low K samples) can cause large age uncertainties which may persist despite the use of the inverse isochron technique. Incremental heating may represent an improved method of analysis in these cases because it has the potential to extract the nonradiogenic component during numerous, well controlled low temperature steps.

In this study, where enough sample was present, one or more aliquots of feldspar was heated at low temperature (1.5-2.5 W) in an attempt to characterize the composition of the nonradiogenic component. In most cases, apparent ages from these low temperature steps

were outside 1σ uncertainties for apparent ages of the 5W steps. Inclusion of the low temperature steps in the inverse isochron commonly resulted in large MSWD. In the 9 cases where inverse isochrons were calculated, exclusion of the 1.5-2.5W analyses resulted in substantial improvement in the MSWD. The low temperature step for D9-22 is typical; it is less radiogenic (higher $^{40}Ar/^{39}Ar$ and $^{36}Ar/^{39}Ar$) and has more K (lower $^{37}Ar/^{39}Ar$) than the 5W steps. In addition, when low temperature steps are included in the York regression, extrapolation yields a different nonradiogenic component composition (e.g., $^{40}Ar/^{36}Ar$ = 325.4) than when only the 5W steps are included. Our results contrast with those of Pringle and others (1991), who show that the nonradiogenic component of their low temperature steps was atmospheric. This difference serves to emphasize the variable behavior of argon in submarine samples.

In general, low temperature steps contrast with associated 5W fusion steps in the following ways: (1) lower radiogenic yield and thus, higher proportion of a nonradiogenic component, (2) lower $^{37}Ar/^{39}Ar$, indicating higher K/Ca for material melting during the 2-2.5W steps, and (3) younger apparent ages. Low temperature steps of samples analyzed by incremental heating commonly have isotopic characteristics different from higher temperature steps (e.g. Fleck and others; 1977, Davis and others, 1989). Explanations for these differences include loss of $^{39}Ar_K$ from alteration products during irradiation (Dalrymple and others, 1987), loss of $^{40}Ar^*$ from alteration phases (Lanphere and Dalrymple, 1978), devitrification (Fleck and others, 1977), or addition of K during alteration (Davis and others, 1989). Perhaps the best explanation for the characteristics of the low temperature steps summarized above is the presence of minor amounts of alteration minerals with high K/Ca (e.g. clays) that preferentially melt during the low temperature steps. This conclusion suggests that alteration products may survive vigorous acid-washing of feldspar separates. Although this proposal is applicable to selected low temperature steps, consideration of low temperature steps for *all* samples in this study suggest that no single phenomenon provides an adequate explanation.

Conclusions

Reliable radiometric ages may be difficult to obtain for submarine samples, especially tholeiitic, low-K_2O basalts. Even alkalic lavas with higher K_2O contents can be difficult to date because some of the K_2O may be secondary (e.g., clay minerals) or the rocks may have excess ^{40}Ar or be contaminated with xenocrysts. The new $^{40}Ar/^{39}Ar$ ages of this study, considered in conjunction with previously published data, indicate that sporadic volcanism occurred in this area from Oligocene to at least late Pleistocene. Most of the edifices appear to be the result of repeated episodes of intraplate volcanism; some edifices are composites of multiple episodes of volcanism that occurred millions of years apart. Although reliable and concordant ages were not obtained for the low-K_2O samples, these small edifices probably originated as off-axis seamounts near the Miocene spreading center. Clearly, more detailed sampling and dating of volcanic edifices in this region are required to determine age distributions and to establish the evolution of these volcanoes in order to gain a better understanding of the magmatic history of this complex region. Available data suggest multiple episodes of chemically diverse volcanism do not fit any simple tectono-magmatic model.

Acknowledgments

We thank J. Hein for providing samples from seamounts offshore southern California; J. Vedder for the samples from the California Borderland, and R. Schmieder for samples from Rocas Alijos. We thank W. Friesen for preparing mineral separates and L.B. Gray for advising and supervising the mineral separations and for reviewing this report. M. Heizler and T. M. Harrison are thanked for their assistance in acquiring and interpreting $^{40}Ar/^{39}Ar$ data.

References

Batiza, R., (1977a), Oceanic crustal evolution: Evidence from the petrology and geochemistry of isolated oceanic central volcanoes: Ph. D. Thesis University of California, San Diego, 295 p.

Batiza, R., (1977b), Petrology and geochemistry of Guadalupe Island: an alkalic seamount on a fossil ridge crest: Geology, v. 5, p. 760-764.

Batiza, R., Bernatowicz, T.J., Hohenberg, C.M., and Podosek, F.A., (1979), Relations of noble gas abundances to petrogenesis and magmatic evolution of some oceanic basalts and related differentiated volcanic rocks: Contributions to Mineralogy and Petrology, v. 69, p. 301-313.

Brooks, C., Hart, S.R., and Wendt, I., (1972), Realistic use of two-error regression treatments as applied to rubidium-strontium data: Rev. Geophys., v. 10, p. 55-557.

Dalrymple G.B., Clague D.A., Vallier T.L., and Menard H.W., (1987), $^{40}Ar/^{39}Ar$ age, petrology and tectonic significance of some seamounts in the Gulf of Alaska. *in* Seamounts, Islands, and Atolls, B.H. Keating, P. Fryer, R. Batiza, and G.W. Boehlert, (eds.) Geophysical Monograph 43, p. 297-318.

Dalrymple G.B., Gromme C.S., and White R.W., (1975), Potassium-argon age and paleomagnetism of diabase dikes in Liberia: Iniation of central Atlantic rifting. Geol. Soc. Amer. Bull., v. 86, p. 399-411.

Dalrymple G.B. and Lanphere M.A., (1971), $^{40}Ar/^{39}Ar$ technique of K-Ar dating: A comparison with the conventional technique. Earth and Planetary Science Letters, v. 12: p. 300-308.

Dalrymple G.B. and Lanphere M.A., (1974), $^{40}Ar/^{39}Ar$ age spectra of some undisturbed terrestrial samples. Geochim Cosmochim. Acta, v. 38: 715-738.

Dalrymple G.B. and Moore J.G., (1968), Argon 40: Excess in submarine pillow basalts from Kilauea Volcano, Hawaii. Science, v. 161, p. 1132-1135.

Davis, A.S., Clague, D.A., Friesen, W.B., and Hein, J.R., 1990, Composition of basaltic glasses dredged from seven seamounts offshore southern California on R/V Farnella cruise F7-87-SC: U.S. Geological Survey Open-File Report 90-53, 21pp.

Davis A.S., Pringle M.S., Pickthorn L.B.G., Clague D.A., (1989), Petrology and age of alkalic lava from the Ratak Chain of the Marshall Islands. Journal of Geophysical Research, v. 94, p. 5757-5774.

Davis, A.S., Siems, D., and Bohrson, W.A., 1994, Petrography, chemistry and age of volcanic rocks from Rocas Alijos; *in* Rocas Alijos, R. Schmieder (ed.), monograph, Kluwer Academic Press, Netherland. (in press).

Fleck R.J., Sutter J.F., and Elliot D.H., (1977), Interpretation of discordant $^{40}Ar/^{39}Ar$ age-spectra of Mesozoic tholeiites from Antarctica. Geochim. Cosmochim. Acta , v.41, p. 15-32.

Hawkins, J.W., Allison, E.C., and Macdougall, D., 1971, Volcanic petrology and geologic history of Northeast Bank, southern California Borderland; Geol. Soc. Amer. Bull., v. 82, p. 219-228.

Honda, M., Bernatowicz, T., Podosek, F.A., Batiza, R., and Taylor, P.T., (1987), Age determinations of eastern Pacific seamounts (Henderson, 6 and 7)--implications for near-ridge and intraplate volcanism: Marine Geology, v. 74, p.79-84.

Lanphere M.A. and Dalrymple G.B., (1978), The use of $^{40}Ar/^{39}Ar$ data in evaluation of disturbed K-Ar systems, Short Papers on the Fourth International Conference of

Geochronology, Cosmochronology, and Isotope Geology, R.E. Zartman (ed.), U.S. Geological Survey Open-File Report 78-701, p. 241-243.

Lonsdale, P., (1991), Structural patterns of the Pacific floor offshore of peninsular California. *in* The gulf and peninsular province of the Californias, Dauphin and others, (eds.): American Association of Petroleum Geologists Memoir, v. 47, p. 87-125.

McDougall, I. and Harrison, T.M., (1988), Geochronology and Thermochronology by the $^{40}Ar/^{39}Ar$ Method, Oxford University Press, New York, 212 pp.

McIntyre, G.A., Brooks, C., Compston, W., and Turek, A., (1966), The statistical assessment of Rb-Sr isochrons: J. Geophys Res, v. 71, p. 5459-5468.

Pringle M.S., Staudigel H., and Gee J., (1991), Geochronology of Jasper Seamount: Seven million years of volcanism. Geology, v. 19, p. 364-368.

Roddick J.C., (1983), High precision intercalibration of ^{40}Ar-^{39}Ar standards. Geochim. Cosmochim. Acta, v. 47, p. 887-898.

Spell, T.L., and Harrison, T.M., (1993), $^{40}Ar/^{39}Ar$ geochronology of post-Valles Caldera rhyolites, Jemez Volcnaic Field, New Mexico: J. Geophy Res: 98, p. 8031-8051.

Steiger R.H. and Jäger E., 1977, Subcommission on geochronology: Convention on the use of decay constants in geo- and cosmochronology. Earth and Planet. Sci. Lett., v. 36, p. 359-362.

Vedder, J.G, 1990, Maps of southern California Continental Borderland showing compositions and ages of bottom samples acquired between 1968 and 1979; U.S. Geological Survey Misc. Field Map, MF-2122, 32 pp.

York D., 1969, Least squares fitting of a straight line with correlated errors. Earth and Planet. Sci. Lett , v. 39, p. 89-93.

Figure captions

Figure 1 Location map for samples from offshore southern and peninsular California.

Figure 2: Inverse isochron diagrams for selected samples. Closed circles are analyses included in inverse isochron regressions, and open circles are excluded analyses. See text for detailed discussion of $^{40}Ar/^{39}Ar$ systematics.

Figure 1

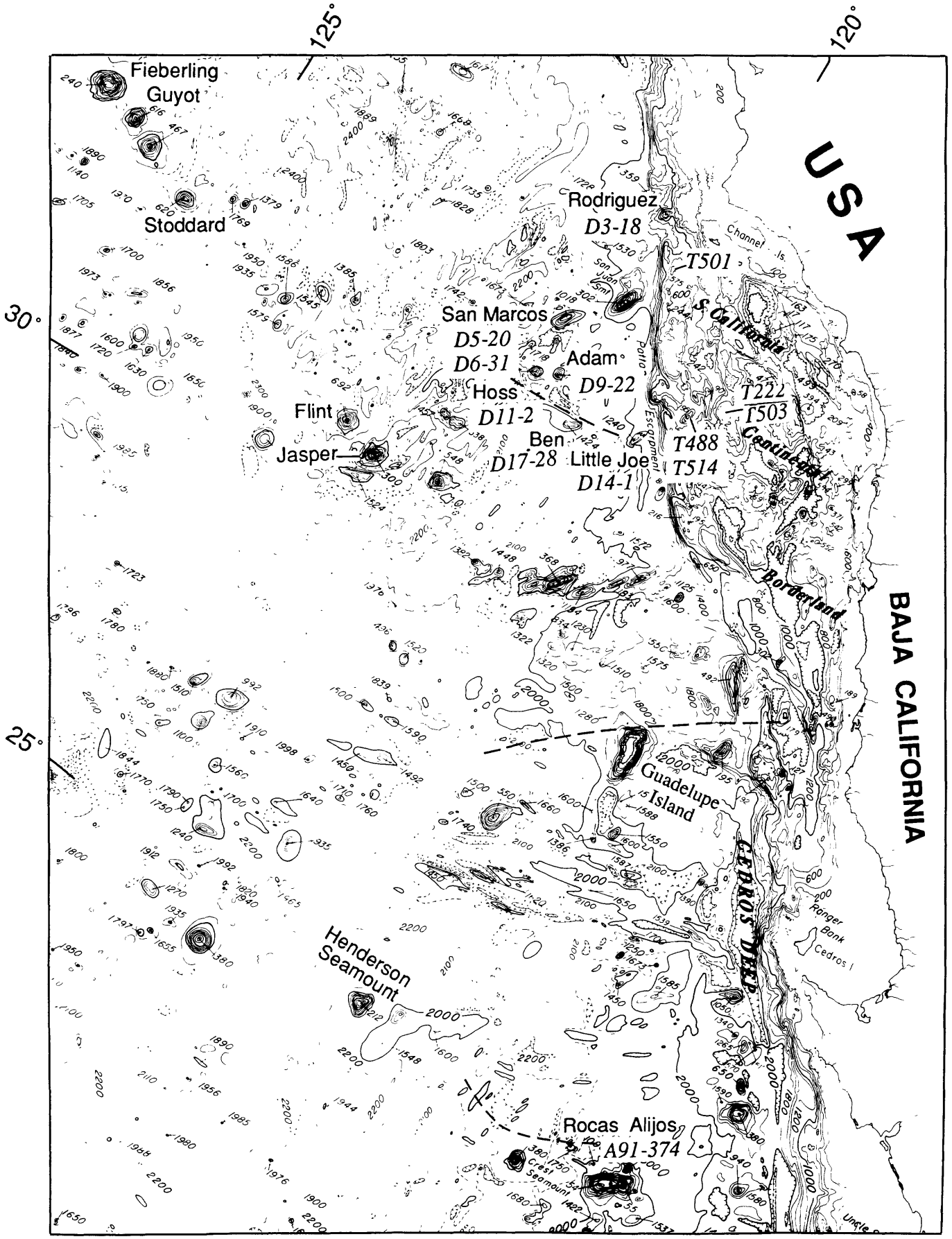
125°
120°
30°
25°
USA
BAJA CALIFORNIA
Fieberling Guyot
Stoddard
Rodriguez
D3-18
T501
San Marcos
D5-20
D6-31
Adam
D9-22
Hoss
D11-2
Flint
Jasper
Ben
D17-28
Little Joe
D14-1
T488
T514
T222
T503
Coronado Escarpment
Coronado Bank
Borderland
Guadelupe Island
CEDROS DEEP
Ranger Bank
Cedros I
Henderson Seamount
Rocas Alijos
A91-374
Crest Seamount
Unnamed

Figure 2

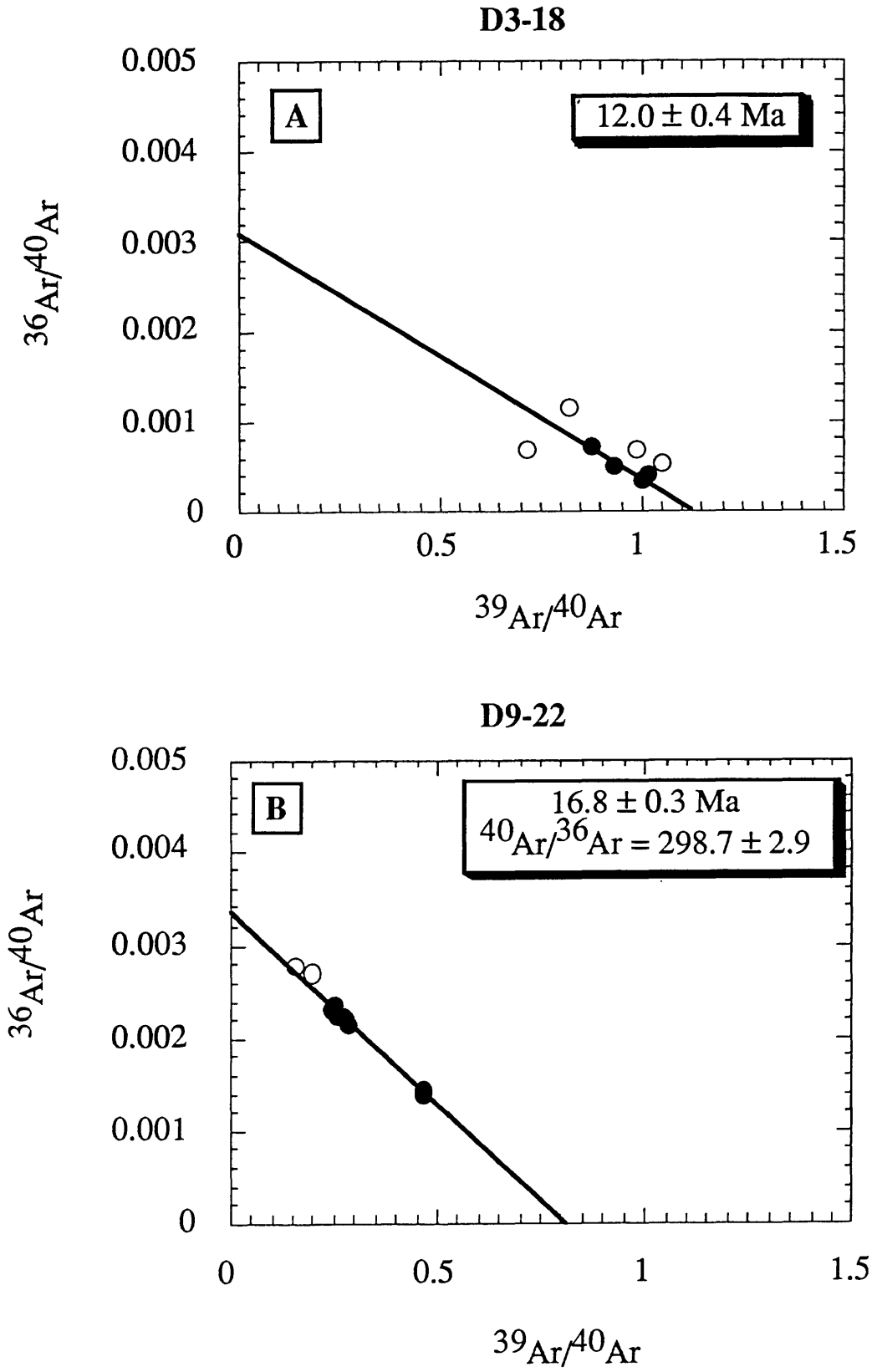
D3-18
A
12.0 ± 0.4 Ma
0.005
0.004
0.003
0.002
0.001
0
0
0.5
1
1.5
36Ar/40Ar
39Ar/40Ar
D9-22
B
16.8 ± 0.3 Ma
40Ar/36Ar = 298.7 ± 2.9
0.005
0.004
0.003
0.002
0.001
0
0
0.5
1
1.5
36Ar/40Ar
39Ar/40Ar

Figure 2 (cont.)

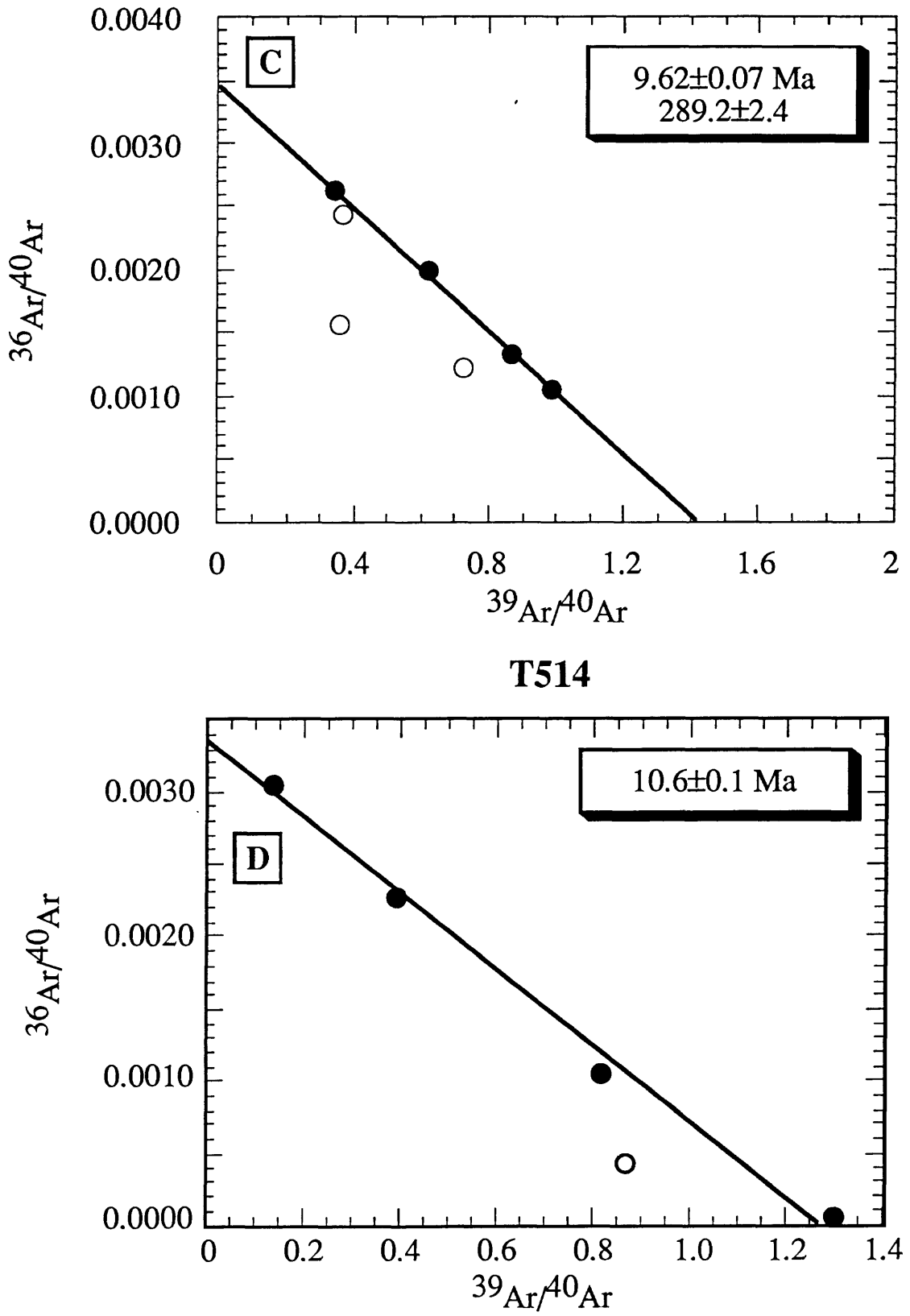

Figure 2 (cont.)

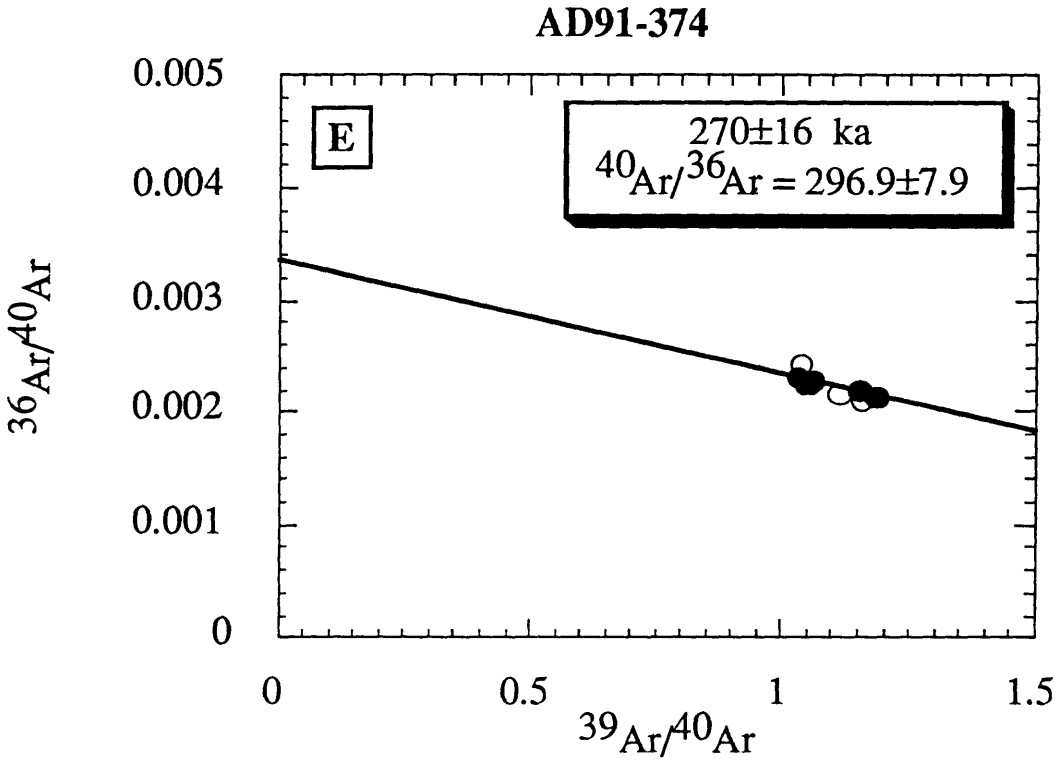

Table 1. Sample Locations

Sample		Location		
		Latitude (N)	Longitude (W)	Water Depth (m)
Offshore Southern California				
D3-18	Rodriguez	34° 00.6'	121° 01.5'	1580 - 1045
D5-20	San Marcos	32° 33.1'	121° 30.3'	4080 - 3045
D6-31	San Marcos	32° 34.5'	121° 32.0'	2305 - 2170
D9-22	Adam	32° 10.6'	121° 16.3'	2300 - 2235
D11-2	Hoss	31° 59.4'	121° 28.5'	2560 - 2540
D14-1	Little Joe	31° 54.6'	120° 44.1'	2925 - 2175
D17-28	Ben	31° 44.2'	120° 44.2'	2925 - 2875
California Borderland				
T222	Tanner Bank	32° 43.1'	119° 12.2'	80
T501	Continental slope	33° 36.9'	120° 40.2'	1050
T503	Tanner Bank	32° 42.1'	119°10.8'	75
T488	Northeast Bank	32° 28.8'	119° 38.1'	1250
T514	Northeast Bank	32° 28.4'	119° 38.6'	1225
Offshore Baja				
A91-374	Rocas Alijos	24° 57.4'	115° 45.8'	80 to +48

Samples from offshore southern California recovered by dredging,
from California Borderland by dart coring, from Rocas Alijos by scuba divers.

Table 2: $^{40}Ar/^{39}Ar$ laser fusion analytical data

Sample	$^{40}Ar/^{39}Ar$[a]	$^{37}Ar/^{39}Ar$[b]	$^{36}Ar/^{39}Ar$ (x 10^{-2})	$^{39}Ar_K$ (x 10^{-14} mol)	$^{40}Ar^*$ (%)	$^{40}Ar^*/^{39}Ar_K$	Age ±1σ (Ma)[c]
Offshore Southern California							
D3-18 J=0.007520							
a	1.085	17.28	0.557	3.34	81.6	0.903	12.2±0.1
b	0.968	18.03	0.576	1.35	79.2	0.794	10.7±0.2
c	1.404	16.72	0.583	3.25	76.9	1.101	14.9±0.1
d	1.153	16.95	0.570	3.11	77.0	0.905	12.2±0.1
f_1	1.031	15.22	0.509	1.50	76.8	0.813	11.0±0.2
f_2	1.010	18.59	0.570	1.29	86.6	0.902	12.2±0.2
g_1	1.237	14.87	0.570	1.18	63.6	0.809	10.9±0.3
g_2	1.003	17.55	0.545	1.65	85.4	0.879	11.9±0.2
D5-20 J=0.007620							
				(x 10^{-15})			
a	31.529	22.96	11.11	5.97	2.0	0.655	9.0±2.8
b_1	74.368	21.67	24.25	1.61	6.1	4.623	62.5±11.5
b_2	31.291	24.92	10.98	2.61	3.1	0.983	13.5±2.4
c_1	19.270	20.92	6.630	1.23	7.5	1.479	20.2±3.4
c_2	18.751	22.56	6.785	8.05	3.2	0.617	8.5±1.2
c_3	5.865	23.92	2.280	4.91	19.2	1.158	15.8±0.8
D6-31 J=0.007620							
a	28.746	23.70	10.15	0.54	2.7	0.778	10.7±2.3
D9-22 J=0.007508							
a	3.811	20.52	1.438	1.62	33.6	1.310	17.7±0.4
b	3.578	21.02	1.390	1.69	34.5	1.262	17.0±0.3
c	3.525	20.31	1.342	1.56	35.8	1.290	17.4±0.3
d	3.999	21.08	1.543	1.33	30.2	1.237	16.7±0.5
e	4.001	21.47	1.540	1.31	31.3	1.283	17.3±0.4
f	3.645	21.56	1.432	1.52	33.5	1.252	16.9±0.3
g_1	6.346	17.14	2.253	5.72	17.6	1.145	15.4±0.8
g_2	2.141	24.23	1.004	9.86	55.9	1.243	16.8±0.4
h_1	5.057	15.91	1.820	4.90	19.6	1.025	13.8±0.5
h_2	2.140	24.20	0.994	1.30	57.3	1.271	17.1±0.4
D11-2 J=0.007620							
				(x 10^{-16})			
a	14.440	320.08	13.12	8.64	20.9	3.959	53.6±5.1
b_1	20.064	245.09	13.11	6.85	11.3	2.778	37.8±13.6
b_2	12.947	403.90	14.51	6.87	35.1	6.483	87.0±7.7
c_1	23.385	278.44	15.11	3.10	10.6	3.181	43.2±13.7
c_2	40.519	274.48	20.69	12.6	7.1	3.568	48.4±6.1
D14-1 J=0.007620							
				(x 10^{-15})			
a	2.662	23.60	1.316	4.15	28.2	0.783	10.7±1.1
b	2.116	22.48	1.200	6.49	21.9	0.476	6.5±2.6
c	2.056	22.30	1.093	4.46	34.0	0.722	9.9±0.8

Table 2: Continued

Sample	$^{40}Ar/^{39}Ar$[a]	$^{37}Ar/^{39}Ar$[b]	$^{36}Ar/^{39}Ar$ (x 10^{-2})	$^{39}Ar_K$ (x 10^{-14} mol)	$^{40}Ar^*$ (%)	$^{40}Ar^*/^{39}Ar_K$	Age ±1σ (Ma)[c]
D17-28 J=0.007594				(x 10^{-15})			
a	1.439	59.29	1.941	6.53	51.7	0.795	10.9±0.5
b	2.484	131.85	4.106	5.42	64.9	1.803	24.5±1.2
c	2.763	153.41	4.868	4.82	54.6	1.707	23.2±1.4
d_1	4.771	127.01	4.828	1.15	28.4	1.524	20.8±3.6
d_2	2.141	187.32	5.515	1.71	84.6	2.176	29.6±2.3
California Borderland							
T222 J= 0.007532			(x10^{-3})				
a	2.433	18.59	5.82	2.24	93.6	2.319	31.2±0.2
b	2.455	18.83	5.92	1.59	92.8	2.326	31.3±0.2
c	2.468	18.41	5.71	1.96	94.0	2.365	31.9±0.2
d	2.420	18.67	5.76	2.01	94.2	2.324	31.3±0.2
e	2.554	18.61	6.06	2.00	90.8	2.365	31.8±0.2
f_1	2.895	18.76	7.99	0.17	68.5	2.148	29.0±0.8
f_2	2.367	18.59	5.51	1.95	96.8	2.337	31.5±0.1
T488 J=0.007583			(x10^{-3})				
a	1.170	14.82	5.82	2.62	59.1	0.702	9.6±0.2
b	1.395	13.04	5.45	3.29	62.5	0.883	12.0±0.2
c	2.920	13.94	11.6	3.14	22.3	0.659	9.0±0.2
d_1	1.623	13.74	7.16	0.80	40.0	0.664	9.1±0.1
d_2	1.033	14.57	5.28	1.59	66.7	0.703	9.6±0.2
e_1	2.774	12.45	7.91	0.66	52.8	1.490	20.3±0.5
e_2	2.724	12.91	10.3	2.63	27.5	0.758	10.3±0.2
T501 J=0.007570			(x10^{-3})				
a	2.440	18.26	5.82	2.20	92.3	2.288	31.0±0.2
b	2.435	18.78	5.71	1.08	95.0	2.361	32.0±0.3
c	2.399	18.67	5.66	1.16	95.3	2.331	31.6±0.3
d	2.388	18.66	5.81	1.01	93.1	2.274	30.8±0.2
e	2.407	17.93	5.54	1.02	94.1	2.308	31.2±0.2
f	2.401	18.58	5.79	0.96	93.4	2.285	30.9±0.5
g_1	2.560	18.76	5.98	0.50	92.1	2.412	32.6±0.3
g_2	2.336	18.76	5.53	1.53	97.3	2.314	31.3±0.2
h_1	3.190	18.85	8.37	0.52	71.6	2.337	31.6±0.4
h_2	2.782	19.10	7.03	1.26	82.8	2.348	31.8±0.3

Table 2: Continued

Sample	$^{40}Ar/^{39}Ar$[a]	$^{37}Ar/^{39}Ar$[b]	$^{36}Ar/^{39}Ar$ (x 10^{-2})	$^{39}Ar_K$ (x 10^{-14} mol)	$^{40}Ar^*$ (%)	$^{40}Ar^*/^{39}Ar_K$	Age ±1σ (Ma)[c]
T503 J=0.007546							
			(x10^{-3})				
a	2.390	18.73	5.83	2.17	93.5	2.276	30.7±0.2
b	2.375	18.67	5.74	1.07	93.9	2.283	30.8±0.3
c	2.395	18.74	5.80	1.12	93.7	2.296	31.0±0.3
d	2.388	18.85	5.77	0.63	93.6	2.305	31.1±0.4
e_1	2.828	18.65	7.11	0.27	78.7	2.332	31.5±0.7
e_2	2.362	18.60	5.64	1.92	95.3	2.293	30.9±0.3
f_1	2.666	18.81	6.71	0.46	83.7	2.309	31.2±0.4
f_2	2.347	18.81	5.62	1.57	96.1	2.302	31.1±0.2
g	2.429	18.70	5.93	1.67	92.2	2.285	30.8±0.2
T514 J=0.007558							
			(x10^{-3})				
a	2.566	14.73	9.98	2.98	33.1	0.900	11.7±0.2
b_1	1.238	14.63	5.48	1.87	67.8	0.900	11.6±0.2
b_2	1.164	14.60	4.60	0.49	85.7	1.000	14.1±0.4
c	0.784	15.19	4.36	1.88	97.1	0.800	10.6±0.2
d	7.520	13.49	26.7	1.70	10.2	0.800	10.6±0.5
Offshore Baja							
AD91-374 J=0.0004850							
		(x 10^{-2})					(ka)
a	0.865	3.029	0.182	1.58	38.0	0.330	289±4
b	0.940	4.242	0.215	3.21	32.9	0.309	270±4
c	0.959	4.746	0.219	3.46	33.1	0.318	278±5
d	0.899	5.226	0.196	3.57	36.1	0.325	284±7
e	0.844	4.680	0.180	3.94	37.2	0.315	275±5
f_1	0.966	6.390	0.236	1.01	28.1	0.274	239±11
f_2	0.867	4.442	0.190	4.40	35.5	0.309	270±5
g	0.842	5.620	0.181	3.57	37.0	0.312	273±5
h	0.947	4.698	0.215	3.63	33.2	0.315	276±4
i	0.971	5.533	0.225	6.69	32.0	0.311	272±3

[a] Background and blank corrected; [b]corrected for ^{37}Ar decay, half life 35.1 days; [c]decay constants taken from Steiger and Jäger (1977), and uncertainties are estimates of the standard deviation of the analytical precision (Dalrymple and Lanphere, 1971). Sample names with subscripts (e.g., f_1) indicate samples typically heated at 2W (1) and melted at 5 W (2). D5-20 was heated in 3 steps: 1.5W (1), 2.5W (2). 5W (3).

Table 3: Summary of $^{40}Ar/^{39}Ar$ ages

Sample	Location	Age of oceanic crust	Inverse isochron age (Ma ±1σ)	$^{40}Ar/^{36}Ar$ (±1σ)	Number of analyses[a]	Weighted mean age (Ma ±1σ)[b]
Offshore Southern California						
D3-18	Rodriguez	18 Ma (Chron 5D)	12.0±0.4	-	4	12.4±0.1
D5-20	San Marcos	20-21 Ma (Chron 6-6A)	16.0±1	299.4±6.0	-	-
D6-31	San Marcos	20-21 Ma (Chron 6-6A)	11±2	-	1	-
D9-22	Adam	21-22 Ma (Chron 6A)	16.8±0.3	298.7±2.9	8	16.8±0.1
D11-2	Hoss	23 Ma (Chron 6B)	-	-	-	-
D14-1	Little Joe	18 Ma (Chron 5D)	-		-	-
D17-28	Ben	20-21 Ma (Chron 6)	<~11(?)	-	-	-
California Borderland						
T222	Tanner Bank	-	31.4±0.1	344±58	4	31.5±0.1
T503	Tanner Bank	-	30.6±0.1	279.6±9.1	9	30.9±0.1
T501	Cont. slope	-	31.2±0.2	304.8±27.5	10	31.4±0.1
T488	NE Bank	-	9.6±0.1	289.2±2.4	4	9.3±0.1
T514	NE Bank	-	10.6±0.1	308.8±12.3	4	11.5±0.1
Offshore Baja						
AD91-374	Rocas Alijos	16 -17 Ma (Chron 5C)	0.270±0.016	296.9±7.9	7	0.275±0.001

[a] refers to the number of analyses used to estimate final age, uncertainty, MSWD, and $^{40}Ar/^{36}Ar$ composition. [b]weighted mean age includes all analyses except for T488, which excludes b and e_1.